

Radiation Synthesis of Organostarch as Fluorescence Label

SHEIKHA A. ALKHURSANI^{1,*}, MOHAMED MOHAMADY GHOBASHY^{2,*} and MOHAMED MADANI¹

¹College of Science and Humanities, Imama Abdulrahman Bin Faisal University, Jubail, Saudi Arabia

²Radiation Research of Polymer Department National Center for Radiation Research and Technology, Atomic Energy Authority, Cairo, Egypt.

*Corresponding authors: E-mail: salkhursani@iau.edu.sa; Mohamed.ghobashy@caea.org.eg

Received: 15 December 2019;

Accepted: 2 May 2020;

Published online: 27 June 2020;

AJC-19951

Fluorescence label preparation, being the core of sensing and imaging, is the most interesting aspect of label technology. Using the gamma irradiation technique, a facial method is proposed to prepare organostarch consisting of polyaniline and starch. Polyaniline was introduced into starch molecules to form an inclusion complex between V-type starch and aniline monomer. The inclusion complex thus formed consisted of starch-aniline crosslink caused by gamma irradiation through organostarch crosslinks. Thus, organostarch develops fluorescence property at 470 nm possibly through the interaction of aniline and starch, which are both fluorophores. A comparative analysis of variations is performed in common fluorescent labels of starch and organostarch based on their physico-chemical properties. X-ray diffraction (XRD) and Fourier transform infrared (FTIR) spectrometry were utilized to confirm the inclusion of polyaniline into starch molecules. Furthermore, using a fluorescence microscope, the positive implementation of fluorescent organostarch was verified. Fluorescent organostarch can be synthesized through this simple method and can be widely used for developing biomarkers and biosensors in food and biomedical industries. Organostarch produces fluorescence under mild conditions even without complicated preparations, such as additives for labelling with dye fluorescence. The intensity of fluorescence of organostarch was 17,000 times that of natural starch.

Keywords: Radiation synthesis, Starch, Organostarch, Fluorescent label.

INTRODUCTION

In plants, starch is present at various places as tiny white granules, for example, in grains (such as sorghum, oat, rice, barley, wheat and maize), seeds of legumes (such as beans and peas), tubers (such as potatoes), stems (such as sago palm), and roots (such as cassava, sweet potatoes, yam and arrowroots) [1]. The main sources of commercial starch are potatoes, cassava, wheat, maize and waxy maize. Similarly, starch is extracted from sweet potatoes, rice, potatoes, arrowroots, sorghum, sago and mung bean [2].

The properties of starch vary considerably based on their sources. The biological origin of starch can be identified from its physical and chemical properties [3]. Furthermore, the properties of starch can be altered through chemical modifications [4]. However, relative differences exist between the intended starches and corresponding modified starches. The properties of the modified starch are influenced by its native properties. Starches can be classified as (i) grain (rice, sorghum, wheat,

maize, *etc.*), (ii) root (tapioca, arrowroot, sweet potato, *etc.*) and tuber (potato) and (iii) waxy (waxy rice, waxy maize, waxy sorghum, *etc.*) starches [5,6]. The structure and properties of the first two starches differ considerably from each another. Although the first and third classes of starch are derived from cereals, the rheological properties of waxy starches are similar to that of tapioca starch. In contrast to potato starch, which has oval granules that are relatively large, maize starch has small polygonal or round granules. The atmospheric temperature and relative humidity determine the water content absorbed by starch granules. Under normal atmospheric conditions, most commercial native starches contain 10-20% moisture [7]. Common starches (sorghum, rice, wheat, maize, *etc.*) contain a higher percentage of fatty substances (0.6-1%) than tapioca (0.1%) and potato (0.05%) starch. The fatty lipid substances are predominantly lysophospholipids in wheat starch and free fatty acids in waxy maize and maize starch. In wheat and maize starches granules, lipids reduce the swelling and the water dissolving capacity of starches [8]. In general, starch molecules

are hydrophobic with a quantum yield of fluorescence. This quantum yield is related to starch hydrophobicity. When starch forms a complex with hydrophobic molecules, such as polyaniline, fluorescence intensity increases with increased hydrophobicity interaction.

Under a fluorescence microscope, starch exhibits intense fluorescence. Starch granules naturally extracted from plant tissues have fluorophore [9]. The native starch has straightforward fluorescence characteristics. Fluorescence imaging is used for observing starch in plant cells [10,11]. For biomedical applications, a fluorescence technique was developed [12]. Generally, fluorescent labelling is performed by using a reactive fluorophore derivative that binds exclusively to a specific group in the target biomolecule [13-15]. A few criteria must be addressed to select a fluorescent probe and labelling technique, *i.e.* (i) fluorescent label must be small sized and chemically stable, with minimal functional groups to bind with the target molecule and (ii) the fluorescent labelling reaction must be highly compact with the target molecule, preferably forming a covalent linkage between the fluorescent label and the target molecule [16].

Starch, being a sustainable resource for industrial applications, is extensively studied [17]. In general, starch is modified for non-food applications [18,19]. However, the literature lacks studies dealing with starch-based fluorescence sensors using fluorescence techniques. Chemically modifying starch through the introduction of organic molecules (π - π^*) may effectively improve starch fluorescence and increase its usability [20,21]. Therefore, we attempted to synthesize a low-cost fluorescent material from starch by using the gamma technique. Gamma irradiation is a promising technique for producing polymeric materials [22-25].

Amylopectin and amylose in starch can form inclusion complexes with other molecules. Amylose can form inclusion complexes with hydrophobic guest molecules, such as aromatic compounds, iodine and fatty acids. Hydrophobic guest molecules change the conformation of amylose from double helix to a single left-handed helix structure called V-amylose [26,27]. Furthermore, in the presence of polyaniline, amylose retains its single helical conformation, forming a V-amylose based on the XRD pattern. V-amylose has a central hydrophobic cavity consisting of a hydrocarbon chain of polyaniline. The guest hydrophobic molecules pass through the amylose helix axis, which has a highly hydrophobic central cavity and a highly hydrophilic outer surface. The hydrophilic property is derived from outer hydroxyl groups. Inclusion complexation binds the inner-cavity hydrophobic molecules more than it does to hydrophobic sites [28,29]. The interactions between guest hydrophobic molecules and amylose molecules form an inclusion complex through the transfer of molecules from a polar environment to a less polar environment [30]. The hydrophobicity of the helical cavity is mandatory for inclusion complex formation.

In this article, a simple method is described for introducing certain organic molecules (polyaniline) into starch molecules to increase its fluorescence without affecting its properties. Polyaniline enhances the optical density of starch through electro donation from π to starch. Fluorescent organic starch can provide

long-term stability and rapid response of the equilibrium, which could be used as a practical polymeric fluorescent probe material.

EXPERIMENTAL

Starch powder was procured from the local market and used as received without further purification. Monomer of aniline 99% from Sigma-Aldrich, Germany.

Fluorescence microscopy: Fluorescence images were obtained using an optical microscope (ZEISS Axio Lab.A1) was used in the excitation wavelengths were 365, 380, 455 and 470 nm while the emission maxima were at 455 nm and 470 nm for blue fluorescence.

Preparation of organostarch samples: Aniline monomer (10 mL) was completely mixed with raw starch powder (10 g). After keeping the mixture standing overnight, it was subjected to 50-kGy gamma radiation. Then, polyaniline/starch powder was washed several times with ethanol/water solvents and unreacted aniline monomer was extracted through filtration. Polyaniline was introduced into starch layers formed after polymerization.

Gamma radiation source: The sample was irradiated at a dose of 1.66 kGy/h with the ^{60}Co Indian irradiation facility gamma rays. The irradiation cell was established by the Egyptian Atomic Energy Authority (AEA) Cairo's National Center for Radiation Research and Technology (NCRRT).

Characterization: The structural characterization and surface morphology of starch and organostarch samples were done by scanning electron microscopy (SEM) 1550 (Leo/Zeiss) was used. The measurements were done with an in-lens detector at 10 kV. APEX™ is EDAX's intuitive and user-friendly 64-bit software program for the collection and analysis of Energy Dispersive Spectroscopy (EDS) data and the compositional characterization of materials. The crystal structure was performed using X-ray diffraction patterns obtained with The XRD-6000 series, including residual austenite quantitation, stress analysis, lattice strain, crystallite size, crystallinity calculation, materials analysis *via* overlaid X-ray diffraction patterns Shimadzu apparatus using nickel-filter and $\text{CuK}\alpha$ Shimadzu Scientific Instruments (SSI), Kyoto, Japan. The chemical structure of starch and organostarch were performed using FTIR-ATR. The Attenuated total reflectance-Fourier transform infrared (ATR-FTIR) is Vertex 70 FTIR model equipped with HYPERION™ series microscope (BrukerOptik GmbH, Ettlingen, Germany) over the 4000-500 cm^{-1} range at a resolution of 4 cm^{-1} was used. Software OPUS 6.0 (Bruker) was used for the data processing.

RESULTS AND DISCUSSION

Proposed mechanism of formation organostarch induced by gamma irradiation: Compared with traditional adsorbents, such as silica gels, bentonites and activated carbons, starch is widely used for adsorbing numerous guest molecules, such as dyes and heavy metals from aqueous solutions. Particularly, no published studies indicate that starch adsorbs aniline. Therefore, this study aimed to prepare starch-aniline crosslinks to produce modified starch called organostarch. Gamma irradi-

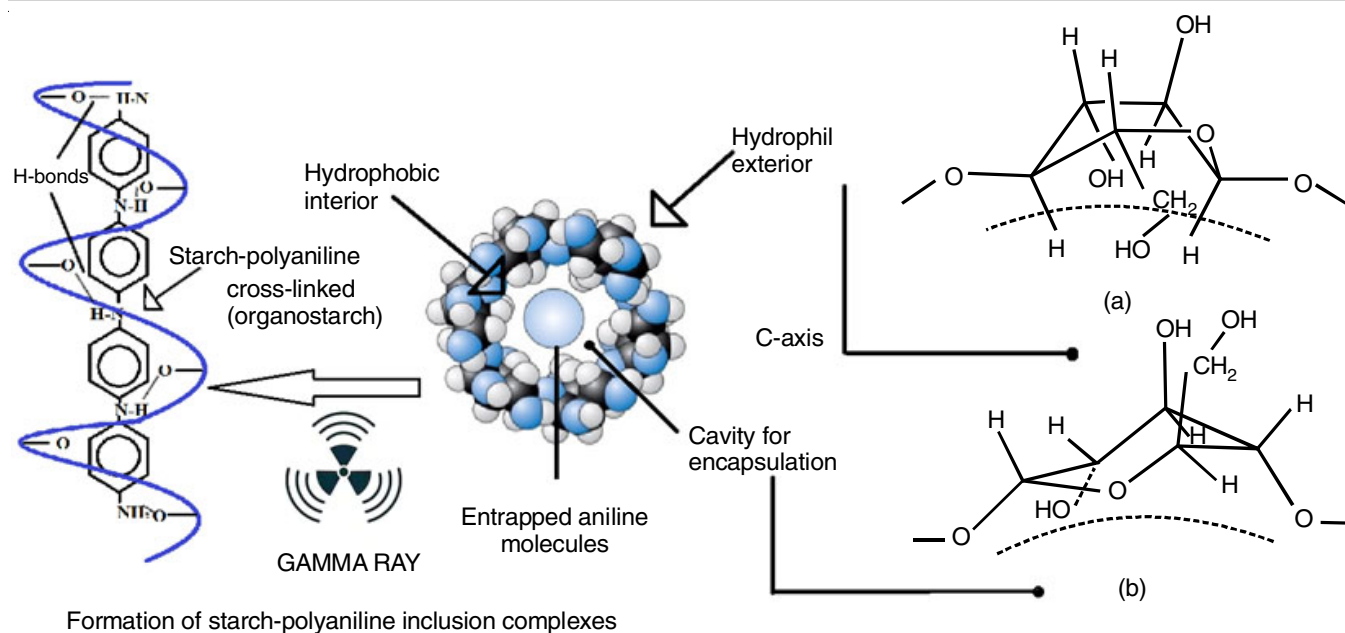


Fig. 1. Proposed mechanism of starch-polyaniline inclusion complexes formation followed by starch polyaniline crosslinked, (a) unstable boat form (b) stable chair form

ation technique was used for initiating and crosslinking starch-aniline. Fig. 1 shows how the starch-aniline inclusion complex forms before gamma irradiation induces starch-polyaniline crosslinks (organostarch). Fig. 1a shows that the glucose molecules arrange themselves to form a stereochemical chair as shown in Fig. 1b, which is more stable than the boat form shown in Fig. 1a. Fig. 1b corresponds to the chemical structure of the amylose helix. The inner structure has a hydrophobic character with three oxygen atoms facing inside and the outer structure has a hydrophilic character. The internal surface of amylose helix binds with hydrocarbon molecules, which leads to amylose affinity with gust hydrophilic molecules (polyaniline).

FTIR analysis: FTIR analysis of starch revealed a characteristic peak due to the stretching vibration of C-H (2929 cm^{-1}). The C-O-H modes of bending at 1078 cm^{-1} ordered the amorphous starch samples [31,32]. The infrared spectrum at 999 cm^{-1} was assigned to glycosidic bonds [33] (Fig. 2). In the organostarch sample, characteristic peaks were observed for polyaniline. The IR peak at 1485 cm^{-1} is attributed to C=C stretching vibrations in the benzene ring and the corresponding C-N peak is observed at 1306 cm^{-1} . The IR peaks at 3280 and 1644 cm^{-1} (attributed to an intermolecular H-bond) have high intensity for organostarch samples (Fig. 2). This is because the O atoms of starch form bonds with H-atoms, with NH groups of aniline molecules along polyaniline chains and the helical axis.

SEM-EDX analysis: SEM-EDX analysis showed that starch and organostarch samples have different surface morphologies. The elemental constituents of starch and organostarch were identified and their positions confirmed through SEM-EDX. The SEM image (Fig. 3a) shows the changes in size and morphology of organostarch granules compared with Fig. 3b. Most of the starch granules are large and oval, with size varying from 10 to $50\text{ }\mu\text{m}$. Chemical modification of starch severely damages these granules (Fig. 3b). Fig. 3a shows that the initial

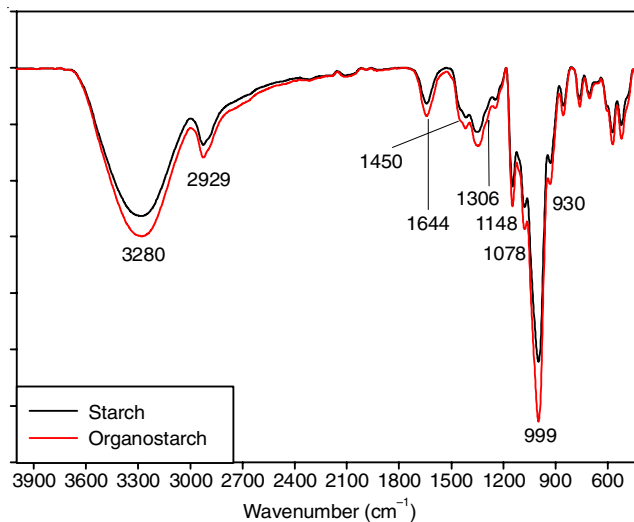


Fig. 2. FTIR spectra of starch and organostarch

granules were approximately $10\text{-}50\text{ }\mu\text{m}$ in diameter, consisting of 63 and $36\text{ wt}\%$ of carbon and oxygen elements, respectively. The chemical modification of starch increased the granules by approximately 20% . Granule sizes of approximately $20\text{-}80\text{ }\mu\text{m}$ in diameter consisted of 54 , 41 and $4\text{ wt}\%$ of carbon, oxygen and nitrogen, respectively (Fig. 3b).

Fluorescence spectra: Fig. 4a shows fluorescence starch granulates before and after polyaniline treatment. Fluorescence intensity was evaluated using imageJ software, which can scan the entire granule surface in pixel steps over the entire granule surface and plot the fluorescence intensity of the area in pixel and frequency. Fig. 4b presents fluorescence intensity *versus* distance, where the blue line indicates organostarch, which is shown to have a higher intensity than natural starch.

Comparison of the fluorescence intensities of organostarch (blue line) and natural starch (pink line) suggest a co-localization.

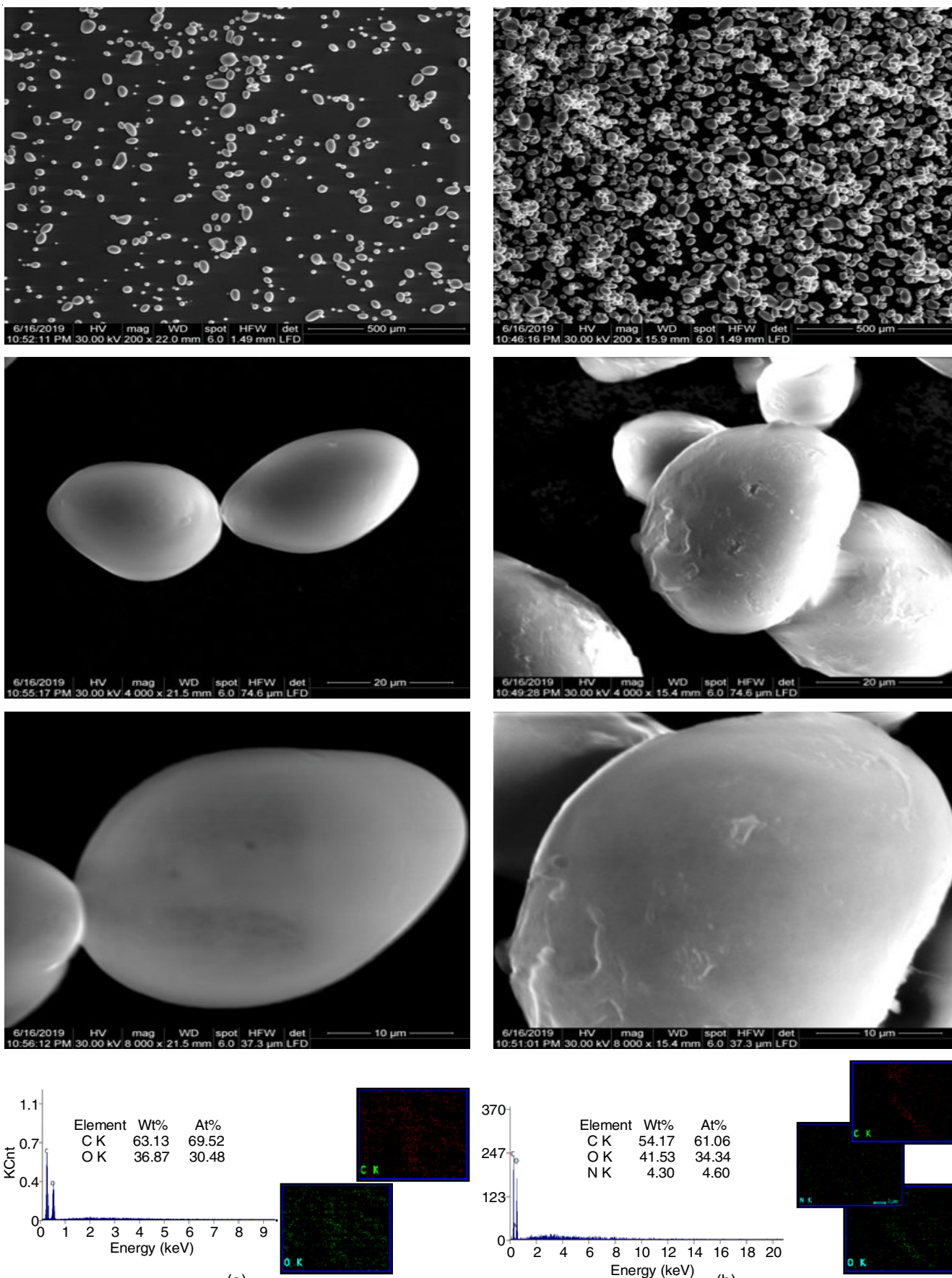


Fig. 3. SEM images and EDX of starch granules (a) and organostarch (b)

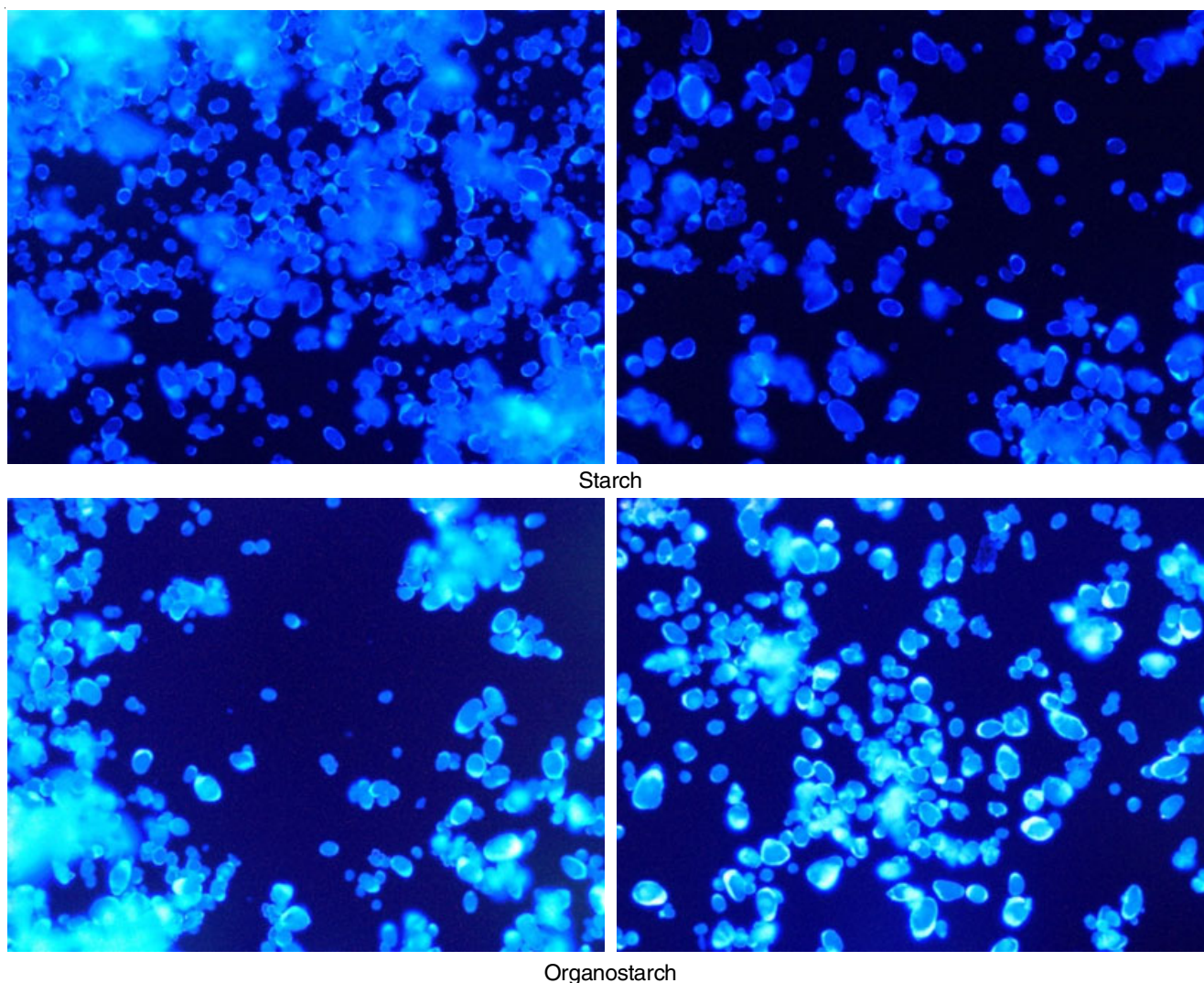


Fig. 4a. Fluorescence image of starch and organostarch

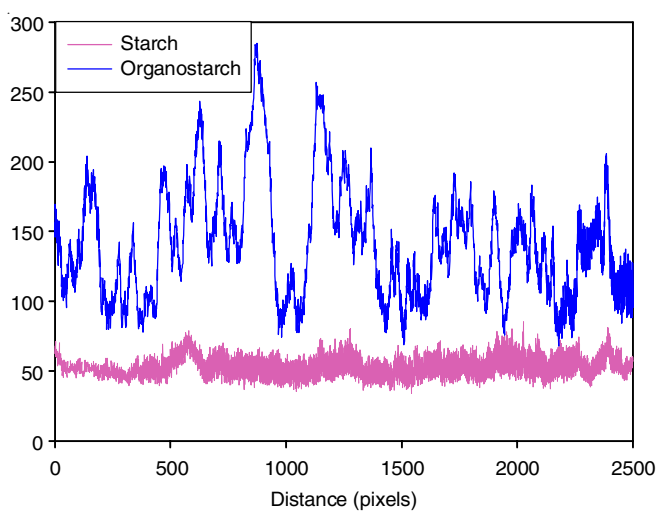


Fig. 4b. Fluorescence intensity profiles of starch and organostarch

Thus, organostarch overlaps two (or more) different fluorescent labels, each with a different emission wavelength, as organostarch has multi-fluorophores in the same pixel. Fig. 4c shows fluorescence intensity *versus* frequency of starch and organo-

starch by using a histogram. The fluorescence intensities of starch and organostarch samples are comparable. Fig. 4c also shows that organostarch exhibits 17,000 times higher fluorescence than starch, which is attributed due to aniline-associated starch molecules.

XRD analysis: XRD indicates starch granules consist to be a mixture of crystalline and amorphous regions. Native starch crystals consist of A-, B- and C-type starches. Fig. 5a shows the XRD patterns of A-, B- and C-type starches. The A-type starch has a characteristic peak at $2\theta = 16.18^\circ$, 17.38° , 30.49° and 33.20° . However, B-type starch has diffraction peaks at $2\theta = 14.18^\circ$ and 9.46° with a weak diffraction peak at $2\theta = 5.73^\circ$. Furthermore, C-type starch has diffraction peaks at $2\theta = 20.00^\circ$, 22.40° and 24.90° [34]. Organostarch produced a typical X-ray pattern of aniline molecules with its major peaks. For crystal planes of PANI in its emeraldine salt form, four distinct peaks appeared at $2\theta = 15.43^\circ$, 21.21° , 25.18° , 32.60° , 33.80° and 41.80° corresponding to (020), (021), (200), (120), (121) and (310), respectively [35,36]. When aniline molecules are introduced into starch molecules, a shift of peaks is caused for A type at 2θ of 17.24° , for B type at 9.62° and for C type at 22.58° and 30.54° .

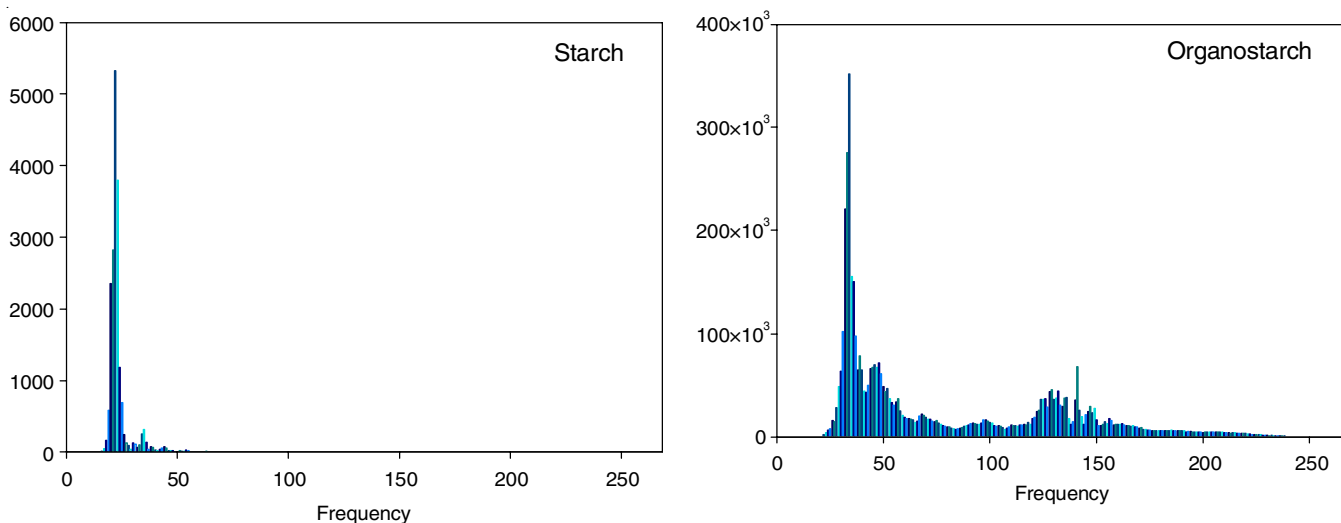


Fig. 4c. Histogram of fluorescence intensity of starch and organostarch

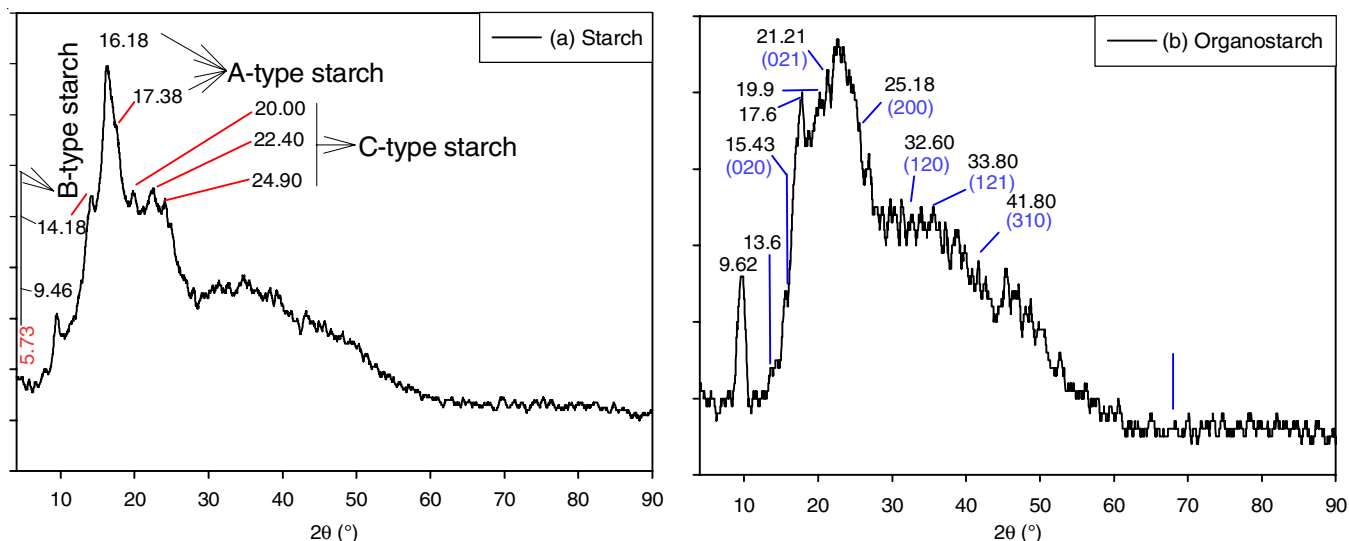


Fig. 5. X-ray diffraction of (a) starch and (b) organostarch

Fig. 5b shows that amylose-polyaniline inclusion complex forms a characteristic XRD peak of V-type starch at 2θ of 12.6° , 17.6° and 19.9° , which are the typical characteristics of an amylose inclusion complex. According to XRD, the peaks of B-type starch disappeared at $2\theta = 5.73^\circ$ (Fig. 5a). Thus, after the starch-polyaniline inclusion complex formation, the characteristic absorption peak of B crystal structure greatly weakened, forming the V-type starch crystal structure [37,38]. XRD revealed that polyaniline molecules induced the formation of amylose single helices, leading to V-complex formation. Thus, aniline molecules change the crystal structure. Therefore, aniline gets distributed inside the starch helix.

Conclusion

In this article, a simple procedure is described of adding certain fluorescent organic molecule (polyaniline) to starch for increasing its fluorescence without affecting its polymer properties. FTIR confirmed that organostarch has intermolecular bonds between H and O atoms of starch, with NH groups of aniline molecules along polyaniline chains and the helical axis.

XRD patterns showed that polyaniline molecules induce the formation of amylose single helices, leading to a V-complex with polyaniline. Thus, aniline molecules become crystalline and well distributed inside the starch helix. Fluorescence microscopy is used for imaging both modified starch and native starch. The polyaniline crosslinking inside starch increase fluorophore union ($\pi-\pi^*$) leading to improved fluorescence properties. Thus, highly stable and long-term fluorescence of organostarch can be obtained.

CONFLICT OF INTEREST

The authors declare that there is no conflict of interests regarding the publication of this article.

REFERENCES

1. S.C. Alcázar-Alay and M.A.A. Meireles, *Food Sci. Technol.*, **35**, 215 (2015); <https://doi.org/10.1590/1678-457X.6749>
2. M. Sapper and A. Chiralt, *Coatings*, **8**, 152 (2018); <https://doi.org/10.3390/coatings8050152>

3. S.G. Haralampu, *Carbohydr. Polym.*, **41**, 285 (2000); [https://doi.org/10.1016/S0144-8617\(99\)00147-2](https://doi.org/10.1016/S0144-8617(99)00147-2)
4. J.M. Fang, P.A. Fowler, C. Sayers and P.A. Williams, *Carbohydr. Polym.*, **55**, 283 (2004); <https://doi.org/10.1016/j.carbpol.2003.10.003>
5. R.L. Whistler, J.N. BeMiller and E.F. Paschall, *Starch: Chemistry and Technology*, Academic Press (2012).
6. N. Singh, J. Singh, L. Kaur, N. Singh Sodhi and B. Singh Gill, *Food Chem.*, **81**, 219 (2003); [https://doi.org/10.1016/S0308-8146\(02\)00416-8](https://doi.org/10.1016/S0308-8146(02)00416-8)
7. R. Hoover, *Crit. Rev. Food Sci. Nutr.*, **50**, 835 (2010); <https://doi.org/10.1080/10408390903001735>
8. J.J.M. Swinkels, *Starke*, **37**, 1 (1985); <https://doi.org/10.1002/star.19850370102>
9. C. Sterling, *Protoplasma*, **59**, 180 (1964); <https://doi.org/10.1007/BF01247861>
10. M. Kokawa, K. Fujita, J. Sugiyama, M. Tsuta, M. Shibata, T. Araki and H. Nabetani, *Biosci. Biotechnol. Biochem.*, **75**, 2112 (2011); <https://doi.org/10.1271/bbb.110342>
11. M. Kokawa, K. Fujita, J. Sugiyama, M. Tsuta, M. Shibata, T. Araki and H. Nabetani, *J. Cereal Sci.*, **55**, 15 (2012); <https://doi.org/10.1016/j.jcs.2011.09.002>
12. S.A. Corr, Y.P. Rakovich and Y.K. Gun'ko, *Nanoscale Res. Lett.*, **3**, 87 (2008); <https://doi.org/10.1007/s11671-008-9122-8>
13. M.S.T. Gonçalves, *Chem. Rev.*, **109**, 190 (2009); <https://doi.org/10.1021/cr0783840>
14. J. Kalia and R.T. Raines, *Curr. Org. Chem.*, **14**, 138 (2010).
15. M.D. Best, *Biochemistry*, **48**, 6571 (2009); <https://doi.org/10.1021/bi9007726>
16. H. Sahoo, *RSC Adv.*, **2**, 7017 (2012); <https://doi.org/10.1039/c2ra20389h>
17. S. Jobling, *Curr. Opin. Plant Biol.*, **7**, 210 (2004); <https://doi.org/10.1016/j.pbi.2003.12.001>
18. A. Para, S. Karolczyk-Kostuch and M. Fiedorowicz, *Carbohydr. Polym.*, **56**, 187 (2004); <https://doi.org/10.1016/j.carbpol.2004.02.001>
19. P. Liu and Z.X. Su, *Carbohydr. Polym.*, **62**, 159 (2005); <https://doi.org/10.1016/j.carbpol.2005.07.018>
20. K. Liu, Y. Wang, H. Li and Y. Duan, *Colloids Surf. B Biointerfaces*, **128**, 86 (2015); <https://doi.org/10.1016/j.colsurfb.2015.02.010>
21. M. Liu, X. Zhang, B. Yang, Z. Li, F. Deng, Y. Yang, X. Zhang and Y. Wei, *Carbohydr. Polym.*, **121**, 49 (2015); <https://doi.org/10.1016/j.carbpol.2014.12.047>
22. A.M. Elbarbary and M.M. Ghobashy, *Carbohydr. Polym.*, **162**, 16 (2017); <https://doi.org/10.1016/j.carbpol.2017.01.013>
23. M.M. Ghobashy, *Ultrason. Sonochem.*, **37**, 529 (2017); <https://doi.org/10.1016/j.ultsonch.2017.02.014>
24. M.M. Ghobashy and M.R. Khafaga, *J. Polym. Environ.*, **25**, 343 (2017); <https://doi.org/10.1007/s10924-016-0805-4>
25. M.M. Ghobashy, *Nanocomposites*, **3**, 42 (2017); <https://doi.org/10.1080/20550324.2017.1316600>
26. G.G. Gelders, T.C. Vanderstukken, H. Goesaert and J.A. Delcour, *Carbohydr. Polym.*, **56**, 447 (2004); <https://doi.org/10.1016/j.carbpol.2004.03.012>
27. W.C. Obiro, S.S. Ray and M.N. Emmambux, *Food Rev. Int.*, **28**, 412 (2012); <https://doi.org/10.1080/87559129.2012.660718>
28. S. Immel and F.W. Lichtenthaler, *Starke*, **52**, 1 (2000); [https://doi.org/10.1002/\(SICI\)1521-379X\(200001\)52:1<1::AID-STAR1>3.0.CO;2-H](https://doi.org/10.1002/(SICI)1521-379X(200001)52:1<1::AID-STAR1>3.0.CO;2-H)
29. J.A. Putseys, L. Lamberts and J.A. Delcour, *J. Cereal Sci.*, **51**, 238 (2010); <https://doi.org/10.1016/j.jcs.2010.01.011>
30. G.F. Fanta, R.L. Shogren and J.H. Salch, *Carbohydr. Polym.*, **38**, 1 (1999); [https://doi.org/10.1016/S0144-8617\(98\)00104-0](https://doi.org/10.1016/S0144-8617(98)00104-0)
31. Q. Liu, G. Charlet, S. Yelle and J. Arul, *Food Res. Int.*, **35**, 397 (2002); [https://doi.org/10.1016/S0963-9969\(01\)00134-X](https://doi.org/10.1016/S0963-9969(01)00134-X)
32. O. Sevenou, S.E. Hill, I.A. Farhat and J.R. Mitchell, *Int. J. Biol. Macromol.*, **31**, 79 (2002); [https://doi.org/10.1016/S0141-8130\(02\)00067-3](https://doi.org/10.1016/S0141-8130(02)00067-3)
33. M. Kacurakova and M. Mathlouthi, *Carbohydr. Res.*, **284**, 145 (1996); [https://doi.org/10.1016/0008-6215\(95\)00412-2](https://doi.org/10.1016/0008-6215(95)00412-2)
34. N.W. Cheetham and L. Tao, *Carbohydr. Polym.*, **36**, 277 (1998); [https://doi.org/10.1016/S0144-8617\(98\)00007-1](https://doi.org/10.1016/S0144-8617(98)00007-1)
35. S.M. Sayyah, M. Shaban and M. Rabia, *Adv. Polym. Technol.*, **37**, 126 (2018); <https://doi.org/10.1002/adv.21649>
36. M. Rabia, H.S.H. Mohamed, M. Shaban and S. Taha, *Sci. Rep.*, **8**, 1107 (2018); <https://doi.org/10.1038/s41598-018-19326-w>
37. Z. Luo, J. Zou, H. Chen, W. Cheng, X. Fu and Z. Xiao, *Carbohydr. Polym.*, **137**, 314 (2016); <https://doi.org/10.1016/j.carbpol.2015.10.100>
38. K. Shamai, H. Bianco-Peled and E. Shimoni, *Carbohydr. Polym.*, **54**, 363 (2003); [https://doi.org/10.1016/S0144-8617\(03\)00192-9](https://doi.org/10.1016/S0144-8617(03)00192-9)